

## From DNA Sequence Analysis to Modeling Replication in the Human Genome

E. B. Brodie of Brodie,<sup>1</sup> S. Nicolay,<sup>1</sup> M. Touchon,<sup>2</sup> B. Audit,<sup>1</sup> Y. d'Aubenton-Carafa,<sup>2</sup> C. Thermes,<sup>2</sup> and A. Arneodo<sup>1</sup>

<sup>1</sup>Laboratoire Joliot-Curie (CNRS), Ecole Normale Supérieure de Lyon, 46 Allée d'Italie, 69364 Lyon Cedex 07, France

<sup>2</sup>Centre de Génétique Moléculaire (CNRS), Allée de la Terrasse, 91198 Gif-sur-Yvette, France

(Received 19 November 2004; published 23 June 2005)

We explore the large-scale behavior of nucleotide compositional strand asymmetries along human chromosomes. As we observe for 7 of 9 origins of replication experimentally identified so far, the (TA + GC) skew displays rather sharp upward jumps, with a linear decreasing profile in between two successive jumps. We present a model of replication with well positioned replication origins and random terminations that accounts for the observed characteristic serrated skew profiles. We succeed in identifying 287 pairs of putative adjacent replication origins with an origin spacing  $\sim 1\text{--}2$  Mbp that are likely to correspond to replication foci observed in interphase nuclei and recognized as stable structures that persist throughout subsequent cell generations.

DOI: 10.1103/PhysRevLett.94.248103

PACS numbers: 87.15.Cc, 87.15.Aa, 87.16.Sr

DNA replication is an essential genomic function responsible for the accurate transmission of genetic information through successive cell generations. According to the “replicon” paradigm derived from prokaryotes [1], this process starts with the binding of some “initiator” protein to a specific “replicator” DNA sequence called origin of replication (*ori*). The recruitment of additional factors initiates the bi-directional progression of two divergent replication forks along the chromosome. One strand is replicated continuously from the origin (leading strand), while the other strand is replicated in discrete steps towards the origin (lagging strand). In eukaryotic cells, this event is initiated at a number of *ori* and propagates until two converging forks collide at a terminus of replication (*ter*) [2]. The initiation of different *ori* is coupled to the cell cycle but there is a definite flexibility in the usage of the *ori* at different developmental stages [3,4]. Also, it can be strongly influenced by the distance and timing of activation of neighboring *ori*, by the transcriptional activity, and by the local chromatin structure [3]. Actually, sequence requirements for an *ori* vary significantly between different eukaryotic organisms. In the unicellular eukaryote *Saccharomyces cerevisiae*, the *ori* spread over 100–150 bp and present some highly conserved motifs [2]. In the fission yeast *Schizosaccharomyces pombe*, there is no clear consensus sequence and the *ori* spread over at least 800 to 1000 bp [2]. In multicellular organisms, the *ori* are rather poorly defined and initiation may occur at multiple sites distributed over thousands of base pairs [5]. Actually, cell diversification may have led higher eukaryotes to develop various epigenetic controls over the *ori* selection rather than to conserve specific replicator sequences [6]. This might explain that only very few *ori* have been identified so far in multicellular eukaryotes, namely, around 20 in metazoa and only about 10 in human [7]. The aim of the present work is to show that with an appropriate coding and an adequate methodology, one can challenge the issue of detecting putative *ori* directly from the genomic sequences.

According to the second parity rule [8], under no-strand bias conditions, each genomic DNA strand should present equimolarities of A and T and of G and C. Deviations from intrastrand equimolarities have been extensively studied in prokaryotic, organelle, and viral genomes for which they have been used to detect the *ori* [9]. Indeed, the GC and TA skews abruptly switch sign at the *ori* and *ter* displaying steplike profiles, such that the leading strand is generally richer in G than in C, and to a lesser extent in T than in A. During replication, mutational events can affect the leading and lagging strands differently, and an asymmetry can result if one strand incorporates more mutations of a particular type or if one strand is more efficiently repaired [9]. In eukaryotes, the existence of compositional biases has been debated and most attempts to detect the *ori* from strand compositional asymmetry have been inconclusive. In primates, a comparative study of the  $\beta$ -globin *ori* has failed to reveal the existence of a replication-coupled mutational bias [10]. Other studies have led to rather opposite results. The analysis of the yeast genome presents clear replication-coupled strand asymmetries in subtelomeric chromosomal regions [11]. A recent space-scale analysis [12] of the GC and TA skews in Mbp long human contigs has revealed the existence of compositional strand asymmetries in intergenic regions, suggesting the existence of a replication bias. Here, we show that the (TA + GC) skew profiles of the 22 human autosomal chromosomes display a remarkable serrated “factory roof”-like behavior that differs from the crenelated “castle rampart”-like profiles resulting from the prokaryotic replicon model [9]. This observation will lead us to propose an alternative model of replication in higher eukaryotes.

Sequences and gene annotation data were downloaded from the UCSC Genome Bioinformatics site and correspond to the assembly of July 2003 of the human genome. To exclude repetitive elements that might have been inserted recently and would not reflect long-term evolutionary patterns, we used the repeat-masked version of the genome leading to a homogeneous reduction of

$\sim 40\%$ – $50\%$  of sequence length. All analyses were carried out using “knowngene” gene annotations. The TA and GC skews were calculated as  $S_{TA} = (T - A)/(T + A)$  and  $S_{GC} = (G - C)/(G + C)$ . Here, we will mainly consider  $S = S_{TA} + S_{GC}$ , since by adding the two skews, the sharp transitions of interest are significantly amplified.

In Fig. 1 are shown the skew  $S$  profiles of three fragments of chromosomes 8 and 20 that contain three experimentally identified *ori*. As commonly observed for eubacterial genomes [9], these three *ori* correspond to rather sharp (over several kbp) transitions from negative to positive  $S$  values that clearly emerge from the noisy background. The leading strand is relatively enriched in T over A and in G over C. The investigation of 6 other known human *ori* [7] confirms the above observation for at least four of them (the two exceptions, namely, the Lamin B2 and  $\beta$ -globin *ori*, might well be inactive in germline cells or less frequently used than the adjacent *ori*). According to the gene environment, the amplitude of the jump can be more or less important and its position more or less localized (from a few kbp to a few tens kbp). Indeed, it is known that transcription generates positive TA and GC skews on the coding strand [13,14], which explains that larger jumps are observed when the sense genes are on the leading strand and/or the antisense genes on the lagging strand, so that replication and transcription biases add to each other. On the contrary to the replicon characteristic steplike profile observed for eubacteria [9],  $S$  is definitely not constant on each side of the *ori* location, making quite elusive the detection of the *ter* since no corresponding downward jumps of similar amplitude can be found in Fig. 1.

In Fig. 2 are shown the  $S$  profiles of long fragments of chromosomes 9, 14, and 21, that are typical of a fair proportion of the  $S$  profiles observed for each chromosome.

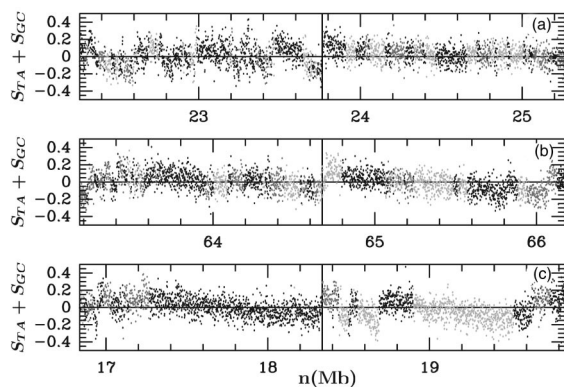


FIG. 1.  $S = S_{TA} + S_{GC}$  vs the position  $n$  in the repeat-masked sequences, in regions surrounding three known human *ori* (vertical bars): (a) MCM4 (native position 48.9 Mbp in chromosome 8 [7(b)]); (b) c-myc (native position 128.7 Mbp in chromosome 8 [7(a)]); (c) TOPI (native position 40.3 Mbp in chromosome 20 [7(c)]). The values of  $S_{TA}$  and  $S_{GC}$  were calculated in adjacent 1 kbp windows. The dark (light) gray dots refer to “sense” (“antisense”) genes with coding strand identical (opposed) to the sequence; black dots correspond to intergenes.

Sharp upward jumps of amplitude ( $\Delta S \sim 0.2$ ), similar to the ones observed for the known *ori* in Fig. 1, seem to exist also at many other locations along the human chromosomes. But the most striking feature is the fact that in between two neighboring major upward jumps, not only the noisy  $S$  profile does not present any comparable downward sharp transition, but it displays a remarkable decreasing linear behavior. At chromosome scale, one thus gets jagged  $S$  profiles that have the aspects of “factory roofs” rather than “castle rampart” steplike profiles as expected for the prokaryotic replicon model [9]. The  $S$  profiles in Fig. 2 look somehow disordered because of the extreme variability in the distance between two successive upward jumps, from spacings  $\sim 50$ – $100$  kbp ( $\sim 100$ – $200$  kbp for the native sequences) up to 2–3 Mbp ( $\sim 4$ – $5$  Mbp for the native sequences) in agreement with recent experimental studies that have shown that mammalian replicons are heterogeneous in size with an average size  $\sim 500$  kbp, the largest ones being as large as a few Mbp [15]. We report in Fig. 3 the results of a systematic detection of upward and downward jumps using the wavelet-transform (WT) based methodology described in Ref. [12(b)]. The selection criterium was to retain only the jumps corresponding to discontinuities in the  $S$  profile that can still be detected with the WT microscope up to the scale 200 kbp which is smaller than the typical replicon size and larger than the typical gene size. In this way, we reduce the contribution of jumps associated with transcription only and maintain a good sensitivity to replication induced jumps. A set of 5100 jumps was detected (with as generally expected an almost equal proportion of upward and downward jumps). In Fig. 3(a) are reported the histograms of the amplitude  $|\Delta S|$  of the so-identified upward ( $\Delta S > 0$ ) and downward ( $\Delta S < 0$ ) jumps, respectively, for the repeat-masked sequences. These histograms do not superimpose, the former being significantly shifted to larger  $|\Delta S|$  values. When plotting  $N(|\Delta S| > \Delta S^*)$  versus  $\Delta S^*$  in Fig. 3(b), one can see that the number of large amplitude upward jumps overexceeds the number of large amplitude downward

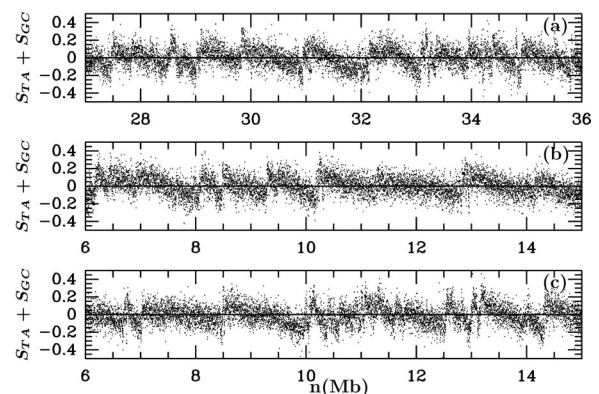


FIG. 2.  $S = S_{TA} + S_{GC}$  skew profiles in 9 Mbp repeat-masked fragments in the human chromosomes 9 (a), 14 (b), and 21 (c). Qualitatively similar but less spectacular serrated  $S$  profiles are obtained with the native human sequences.

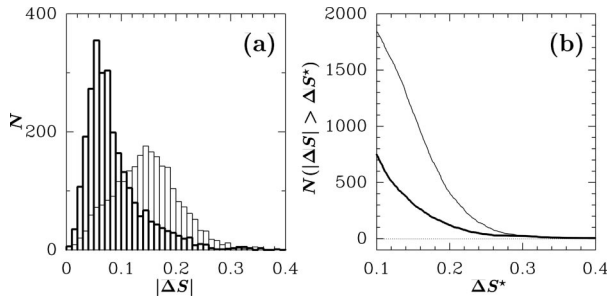


FIG. 3. Statistical analysis of the sharp jumps detected in the  $S$  profiles of the 22 human autosomal chromosomes by the WT microscope at scale  $a = 200$  kbp for repeat-masked sequences [12(b)].  $|\Delta S| = |\bar{S}(3') - \bar{S}(5')|$ , where the averages were computed over the two adjacent 20 kbp windows, respectively, in the 3' and 5' direction from the detected jump location. (a) Histograms  $N(|\Delta S|)$  of  $|\Delta S|$  values. (b)  $N(|\Delta S| > \Delta S^*)$  vs  $\Delta S^*$ . In (a) and (b), the solid (resp. thin) line corresponds to downward  $\Delta S < 0$  (resp. upward  $\Delta S > 0$ ) jumps.

jumps. These results confirm that most of the sharp upward transitions in the  $S$  profiles in Figs. 1 and 2 have no sharp downward transition counterpart. This demonstrates that these jagged  $S$  profiles are likely to be representative of a general asymmetry in the skew profile behavior along the human chromosomes.

As reported in a previous work [14], the analysis of a complete set of human genes revealed that most of them present TA and GC skews and that these biases are correlated to each other and are specific to gene sequences. One can thus wonder to which extent the transcription machinery can account for the jagged  $S$  profiles shown in Figs. 1 and 2. According to the estimates obtained in Ref. [14], the mean jump amplitudes observed at the transition between transcribed and nontranscribed regions are  $|\Delta S_{TA}| \sim 0.05$  and  $|\Delta S_{GC}| \sim 0.03$ , respectively. The characteristic amplitude of a transcription induced transition  $|\Delta S| \sim 0.08$  is thus significantly smaller than the amplitude  $\Delta S \sim 0.20$  of the main upward jumps in Fig. 2. Hence, it is possible that, at the transition between an antisense gene and a sense gene, the overall jump from negative to positive  $S$  values may reach sizes  $\Delta S \sim 0.16$  that can be comparable to the ones of the upward jumps in Fig. 2. However, if some co-orientation of the transcription and replication processes may account for some of the sharp upward transitions in the skew profiles, the systematic observation of “factory roof” skew scenery in intergenic regions as well as in transcribed regions strongly suggests that this peculiar strand bias is likely to originate from the replication machinery. To further examine if intergenic regions present typical “factory roof” skew profiles, we report in Fig. 4 the results of the statistical analysis of 287 pairs of putative adjacent *ori* that actually correspond to 486 putative *ori* almost equally distributed among the 22 autosomal chromosomes. These putative *ori* were identified by (i) selecting pairs of successive jumps of amplitude  $\Delta S \geq 0.12$  and (ii) checking that none of these upward jumps

could be explained by an antisense-gene–sense-gene transition. In Fig. 4(a) is shown the  $S$  profile obtained after rescaling the putative *ori* spacing  $l$  to 1 prior to computing the average  $S$  values in windows of width  $1/10$  that contain more than 90% of intergenic sequences. This average profile is linear and crosses zero at the median position  $n/l = 1/2$ , with an overall upward jump  $\Delta S \simeq 0.17$ . The corresponding average  $S$  profile over windows that are now more than 90% genic is shown in Fig. 4(b). A similar linear profile is obtained but with a jump of larger mean amplitude  $\Delta S \simeq 0.28$ . This is a direct consequence of the gene content of the selected regions. As shown in Fig. 4(b), sense (antisense) genes are preferentially on the left (right) side of the 287 selected sequences, which implies that the replication and—when present—transcription biases tend to add up. In Fig. 4(c) is shown the histogram of the linear slope values of the 287 selected skew profiles after rescaling their length to 1. The histogram of mean absolute deviation from a linear decreasing profile reported in Fig. 4(d) confirms the linearity of each selected skew profiles.

Following these observations, we propose in Fig. 5 a rather crude model for replication that relies on the hypothesis that the *ori* are quite well positioned while the *ter* are randomly distributed. In other words, replication would proceed in a bi-directional manner from well defined ini-

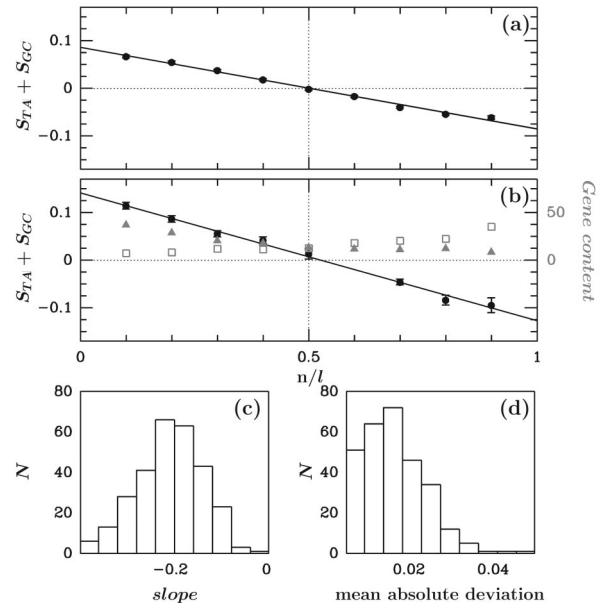


FIG. 4. Statistical analysis of the skew profiles of the 287 pairs of *ori* selected as explained in the text. The *ori* spacing  $l$  was rescaled to 1 prior to computing the mean  $S$  values in windows of width  $1/10$ , excluding from the analysis the first and last half intervals. (a) Mean  $S$  profile ( $\bullet$ ) over windows that are more than 90% intergenic. (b) Mean  $S$  profile ( $\bullet$ ) over windows that are more than 90% genic; the symbols ( $\blacktriangle$ ) [resp. ( $\square$ )] correspond to the percentage of sense (antisense) genes located at that position among the 287 putative *ori* pairs. (c) Histogram of the slope  $s$  of the skew profiles after rescaling  $l$  to 1. (d) Histogram of the mean absolute deviation of the  $S$  profiles from a linear profile.

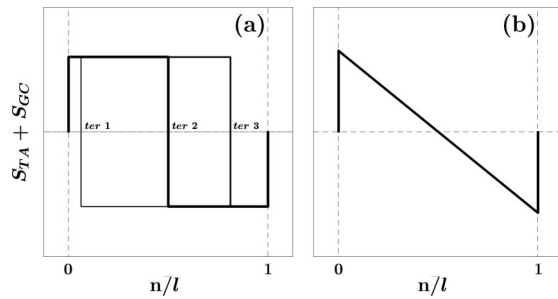


FIG. 5. A model for replication in the human genome. (a) Theoretical skew profiles obtained when assuming that two equally active adjacent *ori* are located at  $n/l = 0$  and 1, where  $l$  is the *ori* spacing; the three profiles in thin, thick, and normal lines correspond to different *ter* positions. (b) Theoretical mean  $S$  profile obtained by summing steplike profiles as in (a), under the assumption of a uniform random positioning of the *ter* in between the two *ori*.

tiation positions, whereas the termination would occur at different positions from cell cycle to cell cycle [16]. Then if one assumes that (i) the *ori* are identically active and (ii) any location in between two adjacent *ori* has an equal probability of being a *ter*, the continuous superposition of steplike profiles like those in Fig. 5(a) leads to the anti-symmetric skew pattern shown in Fig. 5(b), i.e., a linear decreasing  $S$  profile that crosses zero at middle distance from the two *ori*. This model is in good agreement with the overall properties of the skew profiles observed in the human genome and sustains the hypothesis that each detected upward jump corresponds to an *ori*.

To summarize, we have proposed a simple model for replication in the human genome whose key features are (i) well positioned *ori* and (ii) a stochastic positioning of the *ter*. This model predicts jagged skew profiles as observed around most of the experimentally identified *ori* as well as along the 22 human autosomal chromosomes. Using this model as a guide, we have selected 287 domains delimited by pairs of successive upward jumps in the  $S$  profile and covering 24% of the genome. The 486 corresponding jumps are likely to mark 486 *ori* active in the germ line cells. In regards to the rather large size of the selected sequences ( $\sim 2$  Mbp on the native sequence), these putative *ori* are likely to correspond to the large replicons that require most of the  $S$  phase to be replicated [15]. Another possibility is that these *ori* might correspond to the so-called replication foci observed in interphase nuclei [15]. These stable structures persist throughout the cell cycle and subsequent cell generations and likely represent a fundamental unit of chromatin organization. Although the prediction of 486 *ori* seems a significant achievement in regards to the very small number of experimentally identified *ori*, one can reasonably hope to do much better relatively to the large number (probably several tens of thousands) of *ori*. Actually, what makes the analysis quite difficult is the extreme variability of the *ori* spacing from 100 kbp to several Mbp, together with the

necessity of disentangling the part of the strand asymmetry coming from replication from that induced by transcription, a task which is rather delicate in regions with high gene density. To overcome these difficulties, we plan to use the WT with the theoretical skew profile in Fig. 5(b) as an adapted analyzing wavelet. The identification of a few thousand putative *ori* in the human genome would be a very promising methodological step towards the study of replication in mammalian genomes.

This work was supported by the Action Concertée Incitative IMPbio 2004, the Centre National de la Recherche Scientifique, the French Ministère de la Recherche, and the Région Rhône-Alpes.

- 
- [1] F. Jacob, S. Brenner, and F. Cuzin, Cold Spring Harbor Symposia on Quantitative Biology **28**, 329 (1963).
  - [2] S.P. Bell and A. Dutta, Annu. Rev. Biochem. **71**, 333 (2002).
  - [3] S.A. Gerbi and A.K. Bielinsky, Current Opinion in Genetics and Development **12**, 243 (2002); D. Schubeler *et al.*, Nat. Genet. **32**, 438 (2002); D. Fisher and M. Mechali, EMBO J. **22**, 3737 (2003); M. Anglana *et al.*, Cell **114**, 385 (2003).
  - [4] O. Hyrien and M. Mechali, EMBO J. **12**, 4511 (1993).
  - [5] D.M. Gilbert, Science **294**, 96 (2001).
  - [6] J. A. Bogan, D. A. Natale, and M. L. Depamphilis, J. Cell. Physiol. **184**, 139 (2000); M. Méchali, Nat. Rev. Genet. **2**, 640 (2001); C. Demeret, Y. Vassetzky, and M. Méchali, Oncogene **20**, 3086 (2001); A.J. McNairn and D.M. Gilbert, Bioessays (1984-) / BioEssays **25**, 647 (2003); D.M. Gilbert, Nat. Rev. Mol. Cell Biol. **5**, 848 (2004).
  - [7] (a) V. Todorovic, A. Falaschi, and M. Giacca, Front. Biosci. **4**, D859 (1999); (b) E.M. Ladenburger, C. Keller, and R. Knippers, Mol. Cell. Biol. **22**, 1036 (2002); (c) C. Keller *et al.*, J. Biol. Chem. **277**, 31430 (2002); (d) S.M. Cohen *et al.*, J. Cell. Biochem. **85**, 346 (2002); (e) L. Hu, X. Xu, and M. S. Valenzuela, Biochem. Biophys. Res. Commun. **313**, 1058 (2004).
  - [8] J. W. Fickett, D. C. Torney, and D. R. Wolf, Genomics **13**, 1056 (1992); J.R. Lobry, J. Mol. Evol. **40**, 326 (1995).
  - [9] J. Mrazek and S. Karlin, Proc. Natl. Acad. Sci. U.S.A. **95**, 3720 (1998); A. C. Frank and J.R. Lobry, Gene **238**, 65 (1999); E.P. Rocha, A. Danchin, and A. Viari, Mol. Microbiol. **32**, 11 (1999); E.R. Tillier and R. A. Collins, J. Mol. Evol. **50**, 249 (2000).
  - [10] M.P. Francino and H. Ochman, Mol. Biol. Evol. **17**, 416 (2000).
  - [11] A. Gierlik *et al.*, J. Theor. Biol. **202**, 305 (2000).
  - [12] (a) S. Nicolay *et al.*, Phys. Rev. Lett. **93**, 108101 (2004); (b) S. Nicolay *et al.*, Physica A (Amsterdam) **342**, 270 (2004).
  - [13] E. Louis, J. Ott, and J. Majewski, Genome Res. **13**, 2594 (2003).
  - [14] M. Touchon *et al.*, FEBS Lett. **555**, 579 (2003); M. Touchon *et al.*, Nucleic Acids Res. **32**, 4969 (2004).
  - [15] R. Berezney, D.D. Dubey, and J.A. Huberman, Chromosoma **108**, 471 (2000).
  - [16] D. Santamaria *et al.*, Nucleic Acids Res. **28**, 2099 (2000).